Adaptive Robust Precision Motion Control of Systems With Unknown Input Dead-Zones: A Case Study With Comparative Experiments

Chuxiong Hu, *Student Member, IEEE*, Bin Yao, *Senior Member, IEEE*, and Qingfeng Wang

***Abstract*—In this paper, the recently developed integrated direct/indirect adaptive robust control (DIARC) for a class of nonlinear systems with unknown input dead-zones is combined with the desired compensation strategy to synthesize practical high-performance motion controllers for precision electrical drive systems having unknown dead-zone effects. The effect of measurement noise is alleviated by replacing noisy state feedback signals with the desired state needed for perfect output tracking. Theoretically, certain guaranteed robust transient performance and steady-state tracking accuracy are achieved even when the overall system may be subjected to parametric uncertainties, time-varying disturbances, and other uncertain nonlinearities. Furthermore, zero steady-state output tracking error is achieved when the system is subjected to unknown parameters and unknown dead-zone nonlinearity only. The proposed algorithm is also experimentally tested on a linear motor drive system preceded by a simulated unknown nonsymmetric dead-zone. The comparative experimental results obtained validate the necessity of compensating for unknown dead-zone effects and the high-performance nature of the proposed approach.**

***Index Terms*—Adaptive control, dead-zone, linear motor, motion control, nonlinear systems.**

I. Introduction

HIGH-PERFORMANCE control of precision systems has attracted much attention, since designers are likely to encounter a wide range of nonsmooth nonlinearities such as dead-zone [1], [2], hysteresis [3], [4], backlash [5], [6] and friction [7], [8], which could severely deteriorate the achievable control performance, leading to undesirable control accuracy, limit cycles, and even instability [9]. So far, a large number of publications have been devoted to addressing the issue of dead-zone. Specifically, an adaptive dead-zone inverse was proposed in [10], but only bounded output tracking errors are achieved. In [11] and [12], fuzzy logic and neural network were used to provide alternative interpretations to the basis functions needed for adaptive dead-zone inversions [10] but with no essential improvement on theoretically achievable results, i.e., only bounded output tracking errors are obtained. In [13]–[15], the dead-zone was modeled as a combination of a linear input with either an unknown constant gain for symmetric dead-zones or a time-varying unknown gain for nonsymmetric ones and a bounded disturbancelike term. With this formulation, traditional robust adaptive control design techniques can be applied to achieve bounded tracking errors without explicitly exploring the detailed dead-zone characteristics rather than the fact that the dead-zone effect can always be treated as a bounded input disturbance. In [16], smooth basis functions as opposed to the discontinuous ones in [10] were explored to provide some approximate inversions of the dead-zone.

In [17], an integrated direct/indirect adaptive robust control (DIARC) scheme has been developed for a class of single-input–single-output uncertain nonlinear systems preceded by non-symmetrical and non-equal slope dead-zone nonlinearity. The controller makes full use of the dead-zone characteristics that it can be linearly parameterized within certain known working ranges and uses indirect parameter estimation algorithms with online condition monitoring for an accurate estimation of the unknown dead-zone nonlinearity. With these accurate estimates of dead-zone parameters, perfect asymptotic dead-zone compensation is then constructed. Consequently, not only certain guaranteed robust transient performance and final tracking accuracy are preserved, but also asymptotic output tracking has been achieved even in the presence of unknown dead-zone nonlinearity. Asymptotic output tracking was also theoretically achieved in [18] as sliding mode control [19], [20] was employed, but the control inputs included certain chattering problem met in practical implementations. As a result, when stringent practical tracking performance is of major concern, it is often inadequate, as many actual physical systems cannot endure severe chattering inputs [21].

This paper would combine the DIARC scheme in [17] with the desired trajectory compensation to synthesize practical high-performance motion controllers for precision electrical

Manuscript received September 2, 2009; revised January 9, 2010 and April 7, 2010; accepted June 1, 2010. Date of publication August 12, 2010; date of current version May 13, 2011. Part of the paper was presented in the 11th IEEE International Workshop on Advanced Motion Control 2010. This work was supported in part by the U.S. National Science Foundation under Grant CMMI-1052872, by the National Natural Science Foundation of China through the Science Fund for Young Scholars under Grant 50905158, and by the Ministry of Education of China through a Chang Jiang Chair Professorship.

C. Hu is with the State Key Laboratory of Fluid Power Transmission and Control, Zhejiang University, Hangzhou 310027, China, and also with the State Key Laboratory of Tribology, Department of Precision Instruments and Mechanology, Tsinghua University, Beijing 100084, China (e-mail: fyfox.hu@gmail.com).

B. Yao is with the School of Mechanical Engineering, Purdue University, West Lafayette, IN 47907 USA, and also with the State Key Laboratory of Fluid Power Transmission and Control, Zhejiang University, Hangzhou 310027, China (e-mail: byao@purdue.edu).

Q. Wang is with the State Key Laboratory of Fluid Power Transmission and Control, Zhejiang University, Hangzhou 310027, China (e-mail: qfwang@zju.edu.cn).

Color versions of one or more of the figures in this paper are available online at http://ieeexplore.ieee.org.

Digital Object Identifier 10.1109/TIE.2010.2066535

drive systems having unknown dead-zone effects. The resultant controller has several implementation advantages such as less online computation time, reduced effect of measurement noise, and a faster adaptation rate as the noisy state feedback signals are replaced by the desired state needed for perfect output tracking [22], [23]. Theoretically, certain guaranteed robust transient performance and steady-state tracking accuracy are achieved even when the overall system may be subjected to parametric uncertainties, time-varying disturbances, and other uncertain nonlinearities. Furthermore, zero steady-state output tracking is also achieved when the system is subjected to parametric uncertainties and unknown dead-zone nonlinearity only. To validate the effectiveness of the proposed controller, the algorithms are tested on a linear motor drive system preceded by a simulated non-symmetrical and non-equal slope dead-zone nonlinearity, which is assumed to be unknown. Comparative experiments using various controllers such as the existing control algorithm [18], the proposed desired compensation DIARC with no dead-zone compensation, nominal dead-zone compensation, adaptive dead-zone compensation, and complete dead-zone compensation are all carried out. Comparative experimental results show that the DIARC with the proposed adaptive dead-zone compensation outperforms the existing ones [18] significantly—it achieves almost the same tracking performance as that of the DIARC with complete dead-zone compensation. The comparative results also verify the necessity of dead-zone compensation if high-performance tracking is of major concern. Overall, the high-performance tracking results obtained from the experiments validate the effectiveness of the proposed DIARC strategy in practical applications. This control algorithm is also suitable for other types of industrial electric and electronic applications.

II. Problem Statement

A. System Model

System identified frequency responses on a test linear motor drive system illustrate that, within the frequency range of 100 Hz, only the rigid body dynamics of the system need to be considered. In this case, the dynamics of the linear motor preceded by an unknown dead-zone can be described in canonical form as

$$\begin{aligned} \ddot{x} &= Ew(t) - B\dot{x} - AS_f(\dot{x}) + f_u \\ y &= x(t) \quad w(t) = D\left(v(t)\right) \end{aligned} \tag{1}$$

where x represents the position of the inertia load, $v(t)$ is the input to the unknown dead-zone, $w(t)$ represents the control input voltage to the motor, and $y(t)$ is the output from the motor. E is the motor input gain; B is the equivalent viscous friction coefficient; $AS_f(\dot{x})$ represents the nonlinear Coulomb friction, in which amplitude A may be unknown but the continuous shape function $S_f(\dot{x})$ is known; and f_u represents the lumped uncertain nonlinearities including various model approximation errors and external disturbances (e.g., cutting force in machining). The nonlinearity $D(v(t))$ is described as a dead-zone

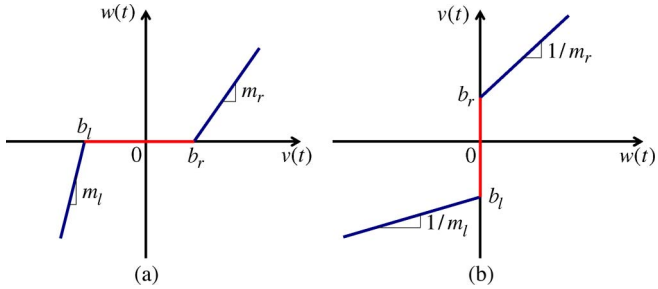

Fig. 1. (a) Dead-zone model. (b) Perfect dead-zone inverse.

characteristic shown in Fig. 1(a). With input $v(t)$ and output $w(t)$, the dead-zone can be represented as in [10] as follows:

$$w(t) = D\left(v(t)\right) = \begin{cases} m_r v(t) - m_r b_r, & \text{for } v(t) \geq b_r \\ 0, & \text{for } b_l < v(t) < b_r \\ m_l v(t) - m_l b_l, & \text{for } v(t) \leq b_l \end{cases} \tag{2}$$

where the parameters m_r, m_l, b_r, and b_l are constants and stand for the right slope, left slope, right break point, and left break point of the dead-zone, respectively.

Set $E = 1$ as the plant input gain E can be considered as a factor of the dead-zone slopes m_r and m_l. For notation simplicity, let $\theta \in R^6$ be the vector of all unknown constant parameters, i.e., $\theta = [B, A, m_r, m_r b_r, m_l, m_l b_l]^{\mathrm{T}}$. The control objective is to design a control law $v(t)$ to ensure that all closed-loop signals are bounded and that the plant state vector $X = [x(t), \dot{x}(t)]$ tracks the specified desired trajectory $X_d = [x_d(t), \dot{x}_d(t)]$, i.e., $X \to X_d$ asymptotically as $t \to \infty$, with certain guaranteed transient responses. The following practical assumptions are made.[1]

Assumption 1: The dead-zone output $w(t)$ is not available for measurement, but the dead-zone parameters m_r, m_l, b_r, and b_l are unknown, and their signs are known as $m_r > 0$, $m_l > 0$, $b_r > 0$, and $b_l < 0$, respectively.

Assumption 2: The unknown parameter vector θ is within a known bounded convex set Ω_θ, i.e., $\forall \theta \in \Omega_\theta$: $B_{\min} \leq B \leq B_{\max}$, $A_{\min} \leq A \leq A_{\max}$, and $0 < m_{r\min} \leq m_r \leq m_{r\max}$, $0 < m_{l\min} \leq m_l \leq m_{l\max}$, $0 < (m_r b_r)_{\min} \leq m_r b_r \leq (m_r b_r)_{\max}$, $(m_l b_l)_{\min} \leq m_l b_l \leq (m_l b_l)_{\max} < 0$, where $B_{\min}$, $B_{\max}$, $A_{\min}$, $A_{\max}$, $m_{r\min}$, $m_{r\max}$, $m_{l\min}$, $m_{l\max}$, $(m_r b_r)_{\min}$, $(m_r b_r)_{\max}$, $(m_l b_l)_{\min}$, and $(m_l b_l)_{\max}$ are all known constants.

Assumption 3: The uncertain nonlinearity f_u satisfies

$$|f_u| \leq \delta(X) f_d(t) \tag{3}$$

where $\delta(X)$ is a known positive function and $f_d(t)$ is an unknown but bounded positive time-varying function.

[1]The following nomenclature is used throughout this paper: $\bullet_{\min}$ and $\bullet_{\max}$ are the minimum and maximum values of $\bullet(t)$ for all t, respectively; $\widehat{\bullet}$ denotes the estimate of $\bullet$; $\widetilde{\bullet} = \widehat{\bullet} - \bullet$ denotes the estimation error, e.g., $\widetilde{\theta} = \widehat{\theta} - \theta$; and $\bullet_i$ is the ith component of vector $\bullet$.

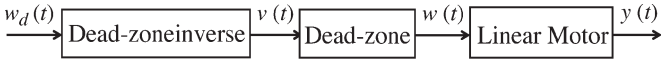

Fig. 2. Controlled system with dead-zone inverse.

B. Dead-Zone Compensation

The essence of compensating the dead-zone effect is to employ a perfect dead-zone inverse function $v(t) = D_I(w(t))$ shown in Fig. 1(b) such that $D(D_I(w(t))) = w(t)\ \forall w(t)$. The following dead-zone inverse will be used:

$$v(t) = \kappa_+(w_d)\frac{w_d(t) + \widehat{(m_r b_r)}}{\widehat{m_r}} + \kappa_-(w_d)\frac{w_d(t) + \widehat{(m_l b_l)}}{\widehat{m_l}} \tag{4}$$

where $\widehat{m_r}$, $\widehat{(m_r b_r)}$, $\widehat{m_l}$, and $\widehat{(m_l b_l)}$ are the estimates of m_r, $m_r b_r$, m_l, and $m_l b_l$, respectively, and w_d is the desired control signal that would achieve the stated control objective when there is no dead-zone effect. Moreover, $\kappa_+(w_d)$ and $\kappa_-(w_d)$ are defined by (5) and (6), respectively, shown at the bottom of the page, where $\widehat{b_r} = \widehat{(m_r b_r)}/\widehat{m_r}$ and $\widehat{b_l} = \widehat{(m_l b_l)}/\widehat{m_l}$. With this dead-zone inverse, the resulting controlled system is shown in Fig. 2.

The proposed DIARC in Section III will use the projection-type adaptation law for all parameter estimates, which guarantees that the dead-zone parameter estimates $\widehat{m_r}$, $\widehat{(m_r b_r)}$, $\widehat{m_l}$, and $\widehat{(m_l b_l)}$ are within their known bounded regions all the time. Thus, in the following, it is implicitly assumed that $\widehat{b_r}(t) > 0$ and $\widehat{b_l}(t) < 0\ \forall t$. With these facts in mind, the following lemma can be obtained.

Lemma 1: With the dead-zone inverse (4), the error between the actual dead-zone output w by (2) and the desired output w_d can be parameterized as

$$\begin{aligned} w - w_d &= \widetilde{(m_r b_r)}\kappa_+(w_d) + \widetilde{(m_l b_l)}\kappa_-(w_d) \\ &- \frac{w_d + \widehat{(m_r b_r)}}{\widehat{m_r}}\widetilde{m_r}\kappa_+(w_d) - \frac{w_d + \widehat{(m_l b_l)}}{\widehat{m_l}}\widetilde{m_l}\kappa_-(w_d) + d(t) \end{aligned} \tag{7}$$

where $d(t)$ is a function defined as

$$\begin{cases} 0, & \text{if } \kappa_+(w_d) = 1 \ \&\ v(t) \geq b_r \\ m_r b_r - \frac{w_d + \widehat{(m_r b_r)}}{\widehat{m_r}} m_r, & \text{if } \kappa_+(w_d) = 1 \ \&\ 0 < v < b_r \\ m_l b_l - \frac{w_d + \widehat{(m_l b_l)}}{\widehat{m_l}} m_l, & \text{if } \kappa_-(w_d) = 1 \ \&\ b_l < v < 0 \\ 0, & \text{if } \kappa_-(w_d) = 1 \ \&\ v(t) \leq b_l \end{cases} \tag{8}$$

and bounded above by

$$\begin{cases} \left|(m_r b_r)_{\max} - \frac{m_{r\min}(m_r b_r)_{\min}}{m_{r\max}}\right|, & \text{if } \kappa_+(w_d) = 1 \\ \left|(m_l b_l)_{\min} - \frac{m_{l\min}(m_l b_l)_{\max}}{m_{l\max}}\right|, & \text{if } \kappa_-(w_d) = 1. \end{cases} \tag{9}$$

In addition, $d(t) \in L_2[0,\infty)$ when $\widetilde{\theta} \in L_2[0,\infty)$, and $d(t) \longrightarrow 0$ when $\widetilde{\theta}(t) \longrightarrow 0$ as $t \longrightarrow \infty$.

Proof: See Appendix A. ■

III. Integrated DIARC Synthesis

In this section, the DIARC strategy [17] will be combined with the desired trajectory compensation [23] for synthesizing $w_d(t)$ in (4) and an online parameter adaptation algorithm for the parameter estimate $\widehat{\theta}$. Consequently, a guaranteed transient and steady-state output tracking performance is attained when other uncertain nonlinearities exist. Furthermore, asymptotic output tracking can finally be achieved as well in the absence of uncertain nonlinearities.

A. Projection-Type Adaptation Law Structure

The widely used projection mapping $Proj_{\widehat{\theta}}$ will be used to keep the parameter estimates within the known bounded set Ω_θ as in [24]. Suppose that the parameter estimate $\widehat{\theta}$ is updated using the following projection-type adaptation law:

$$\dot{\widehat{\theta}} = Proj_{\widehat{\theta}}(\Gamma\tau), \qquad \widehat{\theta}(0) \in \Omega_\theta \tag{10}$$

where τ is any estimation function and $\Gamma(t) > 0$ is any continuously differentiable positive symmetric adaptation rate matrix. With this adaptation law structure, the following desirable properties hold [26].

P1) The parameter estimates are always within the known bounded set Ω_θ, i.e., $\widehat{\theta} \in \Omega_\theta\ \forall t$.

P2)

$$\widetilde{\theta}^T\left(\Gamma^{-1}Proj_{\widehat{\theta}}(\Gamma\tau) - \tau\right) \leq 0 \qquad \forall\tau. \tag{11}$$

B. DIARC Law

With the use of the projection-type adaptation law structure (10), the parameter estimates are bounded with known bounds, regardless of the estimation function τ to be used. In the following, this property will be used to synthesize an integrated DIARC control law for the system (1) that achieves

$$\kappa_+(w_d)(t) = \begin{cases} 1, & \text{if } \left(w_d(t) > 0 \text{ or } \left(w_d(t) = 0\ \&\ \left|v(t_-) - \widehat{b_l}\right| \geq \left|v(t_-) - \widehat{b_r}\right|\right)\right) \\ 0, & \text{else} \end{cases} \tag{5}$$

$$\kappa_-(w_d)(t) = \begin{cases} 1, & \text{if } \left(w_d(t) < 0 \text{ or } \left(w_d(t) = 0\ \&\ \left|v(t_-) - \widehat{b_l}\right| < \left|v(t_-) - \widehat{b_r}\right|\right)\right) \\ 0, & \text{else.} \end{cases} \tag{6}$$

a guaranteed transient and steady-state output tracking accuracy in general. Define

$$s(t) = \dot{\tilde{x}}(t) + \lambda \tilde{x}(t), \quad \text{with} \quad \lambda > 0. \tag{12}$$

Noting (1) and (7) in Lemma 1 as the dead-zone inverse (4) is employed in this scheme, $\dot{s}(t)$ can be derived as

$$\begin{aligned}\dot{s}(t) =& \lambda \dot{\tilde{x}}(t) - \ddot{x}_d(t) - B\dot{x} - AS_f(\dot{x}) + w(t) + f_u \\ =& \lambda \dot{\tilde{x}}(t) - \ddot{x}_d(t) + \varphi\theta_p + w_d(t) + \widetilde{(m_r b_r)}\kappa_+(w_d) \\ &+ \widetilde{(m_l b_l)}\kappa_-(w_d) - \frac{w_d + \widehat{(m_r b_r)}}{\widehat{m_r}}\widetilde{m_r}\kappa_+(w_d) \\ &- \frac{w_d + \widehat{(m_l b_l)}}{\widehat{m_l}}\widetilde{m_l}\kappa_-(w_d) + d(t) + f_u \end{aligned} \tag{13}$$

where $\varphi = [-\dot{x}, -S_f(\dot{x})]$, $\theta_p = [B, A]^{\mathrm{T}}$. The following DIARC function is proposed to design w_d, which would be used in the dead-zone inverse (4) to synthesize the input $v(t)$ as follows:

$$\begin{aligned} w_d =& w_{da} + w_{ds} \\ w_{da} =& w_{da1} + w_{da2} \\ w_{ds} =& w_{ds1} + w_{ds2} \\ w_{da1} =& -\left(\lambda \dot{\tilde{x}}(t) - \ddot{x}_d(t)\right) - \varphi_d \widehat{\theta}_p \\ w_{da2} =& -\widehat{d}_c \\ w_{ds1} =& -k_{s1} s. \end{aligned} \tag{14}$$

In (14), w_{da1} represents the adjustable model compensation with the physical parameter estimates $\widehat{\theta}_p$ updated using an online adaptation algorithm with condition monitoring to be detailed in Section III-C, and $\varphi_d = [-\dot{x}_d, -S_f(\dot{x}_d)]$ is the regressor that depends on the reference trajectory $X_d(t)$ only and is thus free of measurement noise effect. w_{da2} is a model compensation term that is similar to the fast dynamic compensation-type model compensation used in the DIARC designs [24], [27], in which $\widehat{d}_c$ can be thought as the estimate of the low-frequency component of the lumped-model uncertainties defined later. w_{ds} represents the robust control term, in which w_{ds1} is a simple proportional feedback to stabilize the nominal system and w_{ds2} is a robust feedback term used to attenuate the effect of various model uncertainties for a guaranteed robust control performance in general. k_{s1} is a nonlinear gain that is large enough so that

$$\mathbf{Q_1} = \begin{bmatrix} k^\star k_{s1} - k_2 + B + Ag & -\frac{1}{2}\lambda(B + Ag + \lambda) \\ -\frac{1}{2}\lambda(B + Ag + \lambda) & \frac{1}{2}\lambda^3 \end{bmatrix} > 0 \tag{15}$$

where g is defined by $S_f(\dot{x}) - S_f(\dot{x}_d) = g(\dot{x}, t)\dot{\tilde{x}}$, k_2 is any positive constant gain, and $k^\star = \kappa_+(w_d)(m_r/\widehat{m_r}) + \kappa_-(w_d)(m_l/\widehat{m_l})$, which has a value of 1 in the absence of dead-zone slope estimation error. Substituting (14) into (13), $\dot{s}(t)$ can be derived as

$$\begin{aligned}\dot{s}(t) =& (-B - Ag)\dot{\tilde{x}} - \varphi_d \widetilde{\theta}_p + d(t) + f_u \\ &+ \left[\frac{m_r}{\widehat{m_r}}(w_{ds} + w_{da2}) - \frac{\widetilde{m_r}}{\widehat{m_r}} w_{da1} \right. \\ &\left. + \widetilde{(m_r b_r)} - \widetilde{m_r}\frac{\widehat{(m_r b_r)}}{\widehat{m_r}}\right]\kappa_+(w_d) \\ &+ \left[\frac{m_l}{\widehat{m_l}}(w_{ds} + w_{da2}) - \frac{\widetilde{m_l}}{\widehat{m_l}} w_{da1} \right. \\ &\left. + \widetilde{(m_l b_l)} - \widetilde{m_l}\frac{\widehat{(m_l b_l)}}{\widehat{m_l}}\right]\kappa_-(w_d). \end{aligned} \tag{16}$$

Define a constant d_c and time-varying $\triangle^\star(t)$ such that

$$\begin{aligned} d_c + \triangle^\star(t) =& -\varphi_d \widetilde{\theta}_p + d(t) + f_u \\ &- \left[\frac{\widetilde{m_r}}{\widehat{m_r}}\kappa_+(w_d) + \frac{\widetilde{m_l}}{\widehat{m_l}}\kappa_-(w_d)\right] w_{da1} \\ &+ \left[\widetilde{(m_r b_r)} - \widetilde{m_r}\frac{\widehat{(m_r b_r)}}{\widehat{m_r}}\right]\kappa_+(w_d) \\ &+ \left[\widetilde{(m_l b_l)} - \widetilde{m_l}\frac{\widehat{(m_l b_l)}}{\widehat{m_l}}\right]\kappa_-(w_d) \\ =& \vartheta\psi(t) + d(t) + f_u \end{aligned} \tag{17}$$

where $\vartheta = [\widetilde{B}, \widetilde{A}, (\widetilde{m_r}/\widehat{m_r})\kappa_+(w_d) + (\widetilde{m_l}/\widehat{m_l})\kappa_-(w_d), [\widetilde{(m_r b_r)} - \widetilde{m_r}(\widehat{(m_r b_r)}/\widehat{m_r})]\kappa_+(w_d) + [\widetilde{(m_l b_l)} - \widetilde{m_l}(\widehat{(m_l b_l)}/\widehat{m_l})]\kappa_-(w_d)]$, and $\psi(t) = -[-\dot{x}_d, -S_f(\dot{x}_d), w_{da1}, -1]^T$. Conceptually, (17) lumps the original system uncertain nonlinearity f_u with the model uncertainties due to physical parameter estimation errors and divides it into the static component (or low-frequency component in reality) d_c and the high-frequency components $\triangle^\star(t)$. In the following, the low-frequency component d_c will be compensated through fast adaptation that is similar to those in the ARC designs [24], [25] as follows.

Let d_{cM} be any preset bound, and use this bound to construct the following projection-type adaptation law for $\widehat{d}_c$:

$$\dot{\widehat{d}}_c = Proj_{\widehat{d}_c}(\gamma s) = \begin{cases} 0, & \text{if } \left|\widehat{d}_c(t)\right| = d_{cM} \ \& \ \widehat{d}_c s > 0 \\ \gamma s, & \text{else} \end{cases} \tag{18}$$

with $\gamma > 0$ and $\widehat{d}_c(0) = 0$. Such an adaptation law guarantees $|\widehat{d}_c(t)| \le d_{cM}\ \forall t$. Substituting (17) into (16) and noting (14), $\dot{s}(t)$ can be written as

$$\begin{aligned}\dot{s}(t) =& (-B - Ag)\dot{\tilde{x}} + k^\star(w_{ds} + w_{da2}) + d_c + \triangle^\star(t) \\ =& (-B - Ag)\dot{\tilde{x}} + k^\star w_{ds1} + k^\star w_{ds2} - \widetilde{d}_c \\ &+ (1 - k^\star)\widehat{d}_c + \triangle^\star(t). \end{aligned} \tag{19}$$

Noting Assumptions 2 and 3 and P1), there exists a w_{ds2} such that the following two conditions are satisfied:

$$\begin{aligned} &1)\ s w_{ds2} \le 0 \\ &2)\ s\left[k^\star w_{ds2} - \widetilde{d}_c + (1 - k^\star)\widehat{d}_c + \triangle^\star(t)\right] \le \varepsilon + \varepsilon_d f_d^2 \end{aligned} \tag{20}$$

where ε and ε_d are the design parameters, which can be arbitrarily small. Essentially, 2) of (20) shows that w_{ds2} is synthesized to dominate the model uncertainties coming from both parametric uncertainties and uncertain nonlinearities, and 2) is to guarantee that w_{ds2} is dissipative in nature so that it

does not interfere with the functionality of the adaptive control part w_{da}.

Remark 1: One example of w_{ds2} satisfying (20) can be found in the following way. Let h be any function satisfying

$$h \geq |k^{\star}_{\max}|\,|w_{da2}| + \|\vartheta_{\max}\|\|\psi\| + |d(t)|_{\max} \tag{21}$$

where $k^{\star}_{\max} = \max\{(m_{r\max}/m_{r\min}), (m_{l\max}/m_{l\min})\}$, $\vartheta_{1\max} = B_{\max} - B_{\min}$, $\vartheta_{2\max} = A_{\max} - A_{\min}$, $\vartheta_{3\max} = \max\{(m_{r\max} - m_{r\min}/m_{r\min}), (m_{l\max} - m_{l\min}/m_{l\min})\}$, $\vartheta_{4\max} = \max\{(m_r b_r)_{\max} - (m_r b_r)_{\min} + (m_{r\max} - m_{r\min})((m_r b_r)_{\max}/m_{r\min}), (m_l b_l)_{\max} - (m_l b_l)_{\min} - (m_{l\max} - m_{l\min})((m_l b_l)_{\min}/m_{l\min})\}$, and $|d(t)|_{\max} = \max\{|(m_r b_r)_{\max} - m_{r\min}((m_r b_r)_{\min}/m_{r\max})|, |(m_l b_l)_{\min} - m_{l\min}((m_l b_l)_{\max}/m_{l\max})|\}$. Then, choose

$$w_{ds2} = -\left[\frac{1}{4\varepsilon k^{\star}_{\min}}h^2 + \frac{1}{4\varepsilon_d k^{\star}_{\min}}\delta^2(X)\right]s \tag{22}$$

where $k^{\star}_{\min} = \min\{(m_{r\min}/m_{r\max}), (m_{l\min}/m_{l\max})\}$. Using the same techniques in [25], it is easy to show that the aforementioned w_{ds2} satisfies (20).

Theorem 1: When the DIARC control law (14) with the dead-zone inverse (4) and the projection-type adaptation law (10) is applied, regardless of the estimation function τ to be used, in general, all signals in the resulting closed-loop system are bounded, and the output tracking is guaranteed to have a prescribed transient performance and a final tracking accuracy in the sense that the tracking error index s is bounded by

$$V_s \leq e^{-\lambda_v t}V_s^2 + \frac{\varepsilon + \varepsilon_d f^2_{d\max}}{\lambda_v}[1 - e^{-\lambda_v t}] \tag{23}$$

where $V_s = (1/2)s^2 + (1/2)\lambda^2\widetilde{x}^2$, $\lambda_v = \min\{2k_2, \lambda\}$, and $f_{d\max}$ represents the L_∞ norm of the bounded time function $f_d(t)$.

Proof: See Appendix B. ■

C. Parameter Adaptation With Online Condition Monitoring

In the previous subsection, a DIARC control law that can admit any estimation function τ has been constructed, and a guaranteed transient and steady-state tracking performance is achieved as long as the parameter estimates are bounded by the project mapping (10) in accordance with P1). The remainder of this section is to specify suitable parameter adaptation algorithms for τ and Γ so that an improved final tracking accuracy and also asymptotic output tracking can be achieved in the absence of uncertain nonlinearities (i.e., assuming $f_u = 0$ in (1)) with an emphasis on having a good parameter estimation process as well. For this purpose, rather than using any transformed tracking error dynamics to construct the parameter estimation model as in the direct adaptive designs, the actual plant model (1) will be directly used to construct specific estimation functions as detailed hereinafter.

In the following, we will make full use of the fact that, although not being linearly parameterized globally, the unknown dead-zone nonlinearity can be linearly parameterized during the working regions of $v \geq b_r$ or $v \leq b_l$. As such, when the control input $v(t)$ is surely during the regions of $v \geq b_r$ or $v \leq b_l$, indirect parameter estimation algorithms with online condition monitoring can be employed as the parameter adaptation functions for an accurate parameter estimation. In addition, if $v(t)$ is not surely in the regions of $v \geq b_r$ or $v \leq b_l$, the parameter estimation would stop updating until $v(t)$ changes back to these regions. Consequently, accurate estimations of all the unknown dead-zone parameters are possible, and perfect adaptive compensation of unknown dead-zones for asymptotic output tracking is achievable. First, the following lemma must be presented.

Lemma 2: Define a positive constant H as $H = \max\{(m_r b_r)_{\max} - (m_r b_r)_{\min}, (m_l b_l)_{\max} - (m_l b_l)_{\min}\}$. Then, when $|w_d(t)| \geq H$, the dead-zone input $v(t)$ by the proposed dead-zone inverse (4) would satisfy $v(t) \geq b_r$ or $v(t) \leq b_l$.

Proof: See Appendix C. ■

For notation simplicity, define

$$\chi_+(\bullet) = \begin{cases} 1, & \text{if } \bullet > 0 \\ 0, & \text{if else} \end{cases} \quad \chi_-(\bullet) = \begin{cases} 1, & \text{if } \bullet < 0 \\ 0, & \text{if else} \end{cases} \tag{24}$$

and $\chi(w_d(t)) = \chi_+(w_d(t) - H) + \chi_-(w_d(t) + H)$. Then, noting Lemma 2 and multiplying the plant dynamics (1) by $\chi(w_d(t))$, we can get

$$\begin{aligned} \chi(w_d(t))\,\ddot{x} = {} & \chi(w_d(t))\,(-B\dot{x} - AS_f(\dot{x})) \\ & + \chi_+(w_d(t) - H)\,(m_r v(t) - m_r b_r) \\ & + \chi_-(w_d(t) + H)\,(m_l v(t) - m_l b_l) \end{aligned} \tag{25}$$

which is linearly parameterized by the system parameters. Define

$$\begin{aligned} y_\chi(t) &= \chi(w_d(t))\,\ddot{x} \\ F^T(t) &= \chi(w_d(t))\,[-\dot{x}, -S_f(\dot{x}), v(t), -1]\,. \end{aligned} \tag{26}$$

Noting Lemma 2, explicit online condition monitoring can be used to select the measurement data for parameter estimation according to the following two cases.

Case I: First, consider all the measurement data associated with the case when $w_d(t) \geq H$. For this data set, $\chi_+(w_d(t) - H) = 1$ and $\chi_-(w_d(t) + H) = 0$. Thus, the plant dynamics (25) becomes the following linear regression model for parameter estimation:

$$y_\chi(t) = F^T(t)\theta_r \tag{27}$$

where

$$\theta_r = [B, A, m_r, m_r b_r]^{\mathrm{T}} \tag{28}$$

Note that (27) is in standard regression form. With this static model, various estimation algorithms can be used to identify unknown parameters. As it is well known that the least squares estimation algorithm has the best parameter estimation convergence property in general [28], it will be used in the following to estimate the values of θ_r.

In the implementation, since $\ddot{x}$ in (26) is not measured, filtering will be used to obtain all the terms in the estimation model based on the measurement of state X. Namely, let $H_f(s)$

be the transfer function of any stable filter with a relative degree that is larger than or equal to one (e.g., $H_f(s) = 1/(\omega_f s + 1)$). Applying the filter to both sides of (27), we obtain

$$y_{\chi f}(t) = F_f^T(t)\theta_r \tag{29}$$

where $y_{\chi f} = H_f[y_\chi]$ and $F_f = H_f[F]$ can be calculated based on the measurement of state X only. Thus, applying the least squares estimation algorithm with forgetting factor and covariance limiting, the following adaptation function τ is obtained for the estimation of parameter vector θ_r:

$$\tau = -\frac{1}{1 + \upsilon tr\left\{F_f^T \Gamma F_f\right\}} F_f \varsigma \tag{30}$$

where ς and Γ are the prediction error and covariance matrix calculated by

$$\varsigma = F_f^T \widehat{\theta}_r - y_{\chi f} = F_f^T \widetilde{\theta}_r$$
$$\dot{\Gamma} = \begin{cases} \alpha\Gamma - \frac{1}{1+\upsilon tr\left\{F_f^T \Gamma F_f\right\}} \Gamma F_f F_f^T \Gamma, & \text{if } \lambda_{\max}(\Gamma(t)) \le \rho_M \\ 0, & \text{otherwise.} \end{cases} \tag{31}$$

$\alpha \ge 0$ is the forgetting factor, ρ_M is the preset upper bound for the covariance matrix, and $\upsilon \ge 0$, with $\upsilon = 0$ leading to the unnormalized algorithm. The following lemma summarizes the properties of these types of estimators [24], [28].

Lemma 3: With the projection-type adaptation law structure (10) and the least-squares-type adaptation function (30), in the absence of uncertain nonlinearities (i.e., $f_u = 0$ in (1)), if the following persistent excitation (PE) condition is satisfied:

$$\int_t^{t+T} F_f F_f^T d\tau \ge \beta I_p, \text{ for some } \beta > 0 \text{ and } T > 0 \tag{32}$$

then the estimates of physical parameters $\widehat{\theta}_r$'s converge to their true values, i.e., $\widetilde{\theta}_r(t) \to 0$ as $t \to \infty$.

Case II: Now, consider all the measurement data associated with the case when $w_d(t) \le -H$. For this data set, $\chi_+(w_d(t) - H) = 0$ and $\chi_-(w_d(t) + H) = 1$, and the plant dynamics (25) becomes the following linear regression model for parameter estimation:

$$y_\chi(t) = F^T(t)\theta_l \tag{33}$$

where

$$\theta_l = [B, A, m_l, m_l b_l]^{\mathrm{T}}. \tag{34}$$

Thus, the same procedure as that in Case I can be used to estimate the physical parameter set θ_l, and the estimates $\widehat{\theta}_l$'s converge to their true values, i.e., $\widetilde{\theta}_l(t) \to 0$ as $t \to \infty$, when a certain PE condition like (32) is satisfied. The details are omitted as they are identical to those in Case I.

Overall, the parameter estimations of Cases I and II guarantee that all unknown physical parameters, i.e., $\theta = [B, A, m_r, m_r b_r, m_l, m_l b_l]^{\mathrm{T}}$, are accurately estimated, provided that the PE conditions like (32) are satisfied.

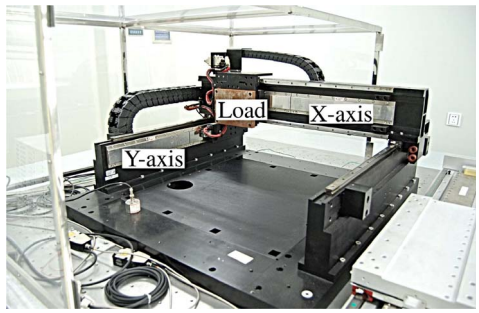

Fig. 3. Biaxial linear motor-driven gantry system.

D. Asymptotic Output Tracking

With the accurate parameter estimates obtained in Section III-C, in addition to Theorem 1, an improved steady-state tracking performance is also obtained as follows.

Theorem 2: In the absence of uncertain nonlinearities (i.e., assuming $f_u = 0$ in (1)), when the PE conditions like (32) are satisfied, the DIARC control law (14) with the dead-zone inverse (4) and the projection-type adaptation law (10) and (30) can achieve an improved steady-state tracking performance—asymptotic output tracking, i.e., $\widetilde{X}(t) \to 0$ and $s \to 0$ as $t \to \infty$.

Proof: See Appendix D. ■

IV. Comparative Experiments

The proposed DIARC control algorithm is implemented on the Y-axis of a precision X–Y Anorad HERC-510-510-AA1-B-CC2 gantry driven by LC-50-200 iron core linear motors, as shown in Fig. 3. The position sensors of the gantry are two linear encoders with a resolution of 0.5 μm after quadrature. The velocity signal is obtained by the difference of two consecutive position measurements. Standard offline least squares identification is performed to obtain the parameters of the Y-axis. To test the learning capability of the proposed DIARC algorithms, a 5-kg load is mounted on the motor in the experiments, and the identified values of the parameters are $B = 0.8/s$, $A = 0.23/s$, $E = 1.55$ m/s^2/V, and $f_N = 0$ m/s^2, where f_N is the nominal value of f_u. All the control algorithms are implemented using a dSPACE DS1103 controller board. The controller executes programs at a sampling period of $T_s = 0.2$ ms, resulting in a velocity measurement resolution of 0.0025 m/s. The control objective is to let the system state $[x, \dot{x}]^{\mathrm{T}}$ follow its desired trajectory $[x_d, \dot{x}_d]^{\mathrm{T}}$. Assuming

$$x_d = 0.21 + 0.08\sin(\pi t - \pi/2) + 0.07\sin(0.8\pi t - \pi/2) + 0.06\sin(1.2\pi t - \pi/2) \tag{35}$$

the initial values of plant states are set as $X(0) = [0, 0]^{\mathrm{T}}$.

A. Comparative Experiment I

Suppose that $w(t)$ is the output of a simulated dead-zone described by

$$w = D(v) = \begin{cases} 0.9(v-1.2), & \text{for } v \geq 1.2 \\ 0, & \text{for } -1 < v < 1.2 \\ 1\,(v-(-1)), & \text{for } v \leq -1 \end{cases} \quad (36)$$

which is practically supposed to be unknown and precede the input of the linear motor. Adding the effect of $E = 1.55$ m/s^2/V into the dead-zone, we can describe the dead zone as

$$w = D(v) = \begin{cases} 1.395v - 1.674, & \text{for } v \geq 1.2 \\ 0, & \text{for } -1 < v < 1.2 \\ 1.55v + 1.55, & \text{for } v \leq -1. \end{cases} \quad (37)$$

Thus, the approximate accurate values are $\theta = [0.8, 0, 23, 1.395, 1.674, 1.55, -1.55]^{\mathrm{T}}$. As the simulated dead-zone is supposed to be unknown, we set the nominal values to be $\theta_N = [0.8, 0, 23, 1.6, 1.8, 1.8, -1.4]^{\mathrm{T}}$. The bounds of the parametric variations are chosen as

$$\theta_{\min} = [0.7, 0.1, 1.2, 1.4, 1.2, -1.8]^{\mathrm{T}}$$
$$\theta_{\max} = [1, 0.4, 1.7, 1.9, 1.9, -1.2]^{\mathrm{T}}. \quad (38)$$

To better illustrate the effectiveness of the proposed scheme, particularly the dead-zone compensation, the following control algorithms for system (1) are implemented and compared.

- C1) The proposed DIARC adapting the estimates of physical parameters B, A, E, and f_N and ignoring the existence of the unknown dead-zone (36). This case represents the scenario where the existence of dead-zone is totally ignored.
- C2) The proposed DIARC adapting the estimates of physical parameters B, A, E, and f_N only and without updating the dead-zone parameter estimates. This case represents the scenario where the dead-zone is compensated with their nominal values and the effects of the unknown dead-zone are ignored.
- C3) The proposed DIARC presented in Sections II and III.
- C4) The proposed DIARC in which only B, A, E, and f_N are updated based on the proposed online parameter adaptation algorithm and the dead-zone (36) effect is compensated by (4) with actual dead-zone parameter values assuming that the dead-zone parameters are known. Thus, this case represents the ideal scenario where the dead-zone effect can be completely compensated.

In C3), w_{ds2} in (14) is given in Section III-B. Theoretically, we should use the form of $w_{ds2} = -k_{s2}s$, with k_{s2} being a nonlinear proportional feedback gain, as given in (22), to satisfy the robust performance requirement (20) globally. In the implementation, a large-enough constant feedback gain k_{s2} is used instead to simplify the resulting control law. With such a simplification, although the robust performance condition (20) may not be guaranteed globally, the condition can still be satisfied in a large-enough working range, which might be acceptable to practical applications, as done in [27], [29], and [30]. With this simplification, noting (14), we choose $w_{ds} = -k_s s$ in the experiments where k_s represents the summation of k_{s1} and k_{s2} and is chosen as $k_s = 200$. The constant λ in (12) is selected as $\lambda = 200$. The constant adaptation rate γ in (18) is set as $\gamma = 1000$, and the bound of $\widehat{d}_c$ is chosen to be $d_{cM} = 2$. The initial values of all parameter estimates are $\widehat{\theta}(0) = [0.8, 0, 23, 1.6, 1.8, 1.8, -1.4]^{\mathrm{T}}$, which are chosen to be the same as the nominal values θ_N's. The initial value of the adaptation matrix Γ in (30) is $\Gamma(0) = 1000I_6$, and the forgetting factor is chosen as $\alpha = 0.1$. The constant H in Lemma 2 is set as $H = 0.7$. For a fair comparison, the controller parameters and the initial values in cases C1, C2, and C4 are chosen the same as that in C3 when they have the same meaning (e.g., w_{ds} in C1, C2, and C4 are chosen the same as that in C3). The initial values of the adaptation matrix Γ in (30) for C1, C2, and C4 are $\Gamma(0) = 1000I_4$, for which the dead-zone parameters are not adapted; consequently, there are B, A, E, and f_N those need to be estimated, and their initial values are $[0.8, 0.23, 1.55, 0]^{\mathrm{T}}$. In C4, the dead-zone (36) is known and can be completely compensated by its inverse (4).

TABLE I
PERFORMANCE INDEXES OF COMPARATIVE EXPERIMENTS I AND II

	Experiments I				Experiments II	
Controller	C1	C2	C3	C4	C5	C3
$\|\|\widetilde{x}\|\|_2(\mu m)$	23.41	8.25	2.70	2.64	31.19	2.77
$\|\|\widetilde{x}\|\|_\infty(\mu m)$	84.04	29.55	9.95	9.96	65.16	10.00

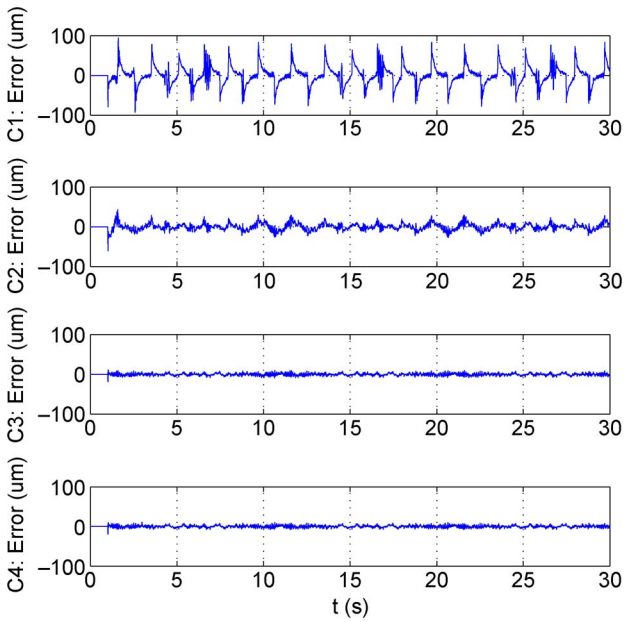

Fig. 4. Output tracking errors of DIARCs with dead-zone.

The experimental results in terms of some performance indexes after running the gantry for one period are given in Experiment I of Table I. Overall, C2, C3, and C4 achieve good steady-state tracking performances during movements, which are better than that in C1. C3 and C4 achieve almost the same excellent tracking performances that are better than that in C2. The experimental results for all four controllers are shown in Figs. 4–7. Specifically, Fig. 4 shows the tracking errors of all

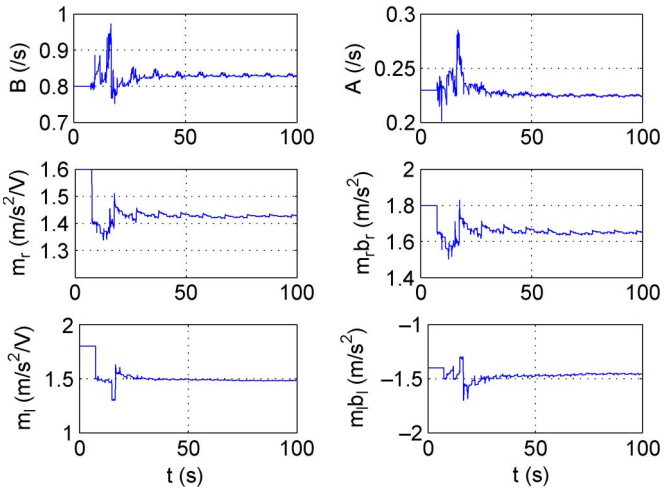

Fig. 5. Parameter estimates of DIARC in C3.

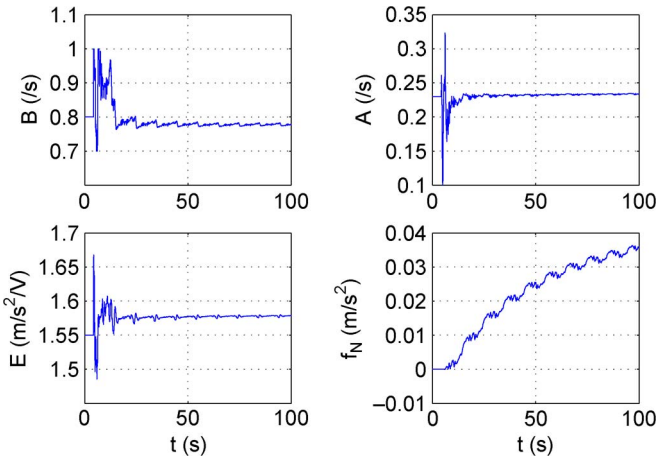

Fig. 6. Parameter estimates of DIARC in C4.

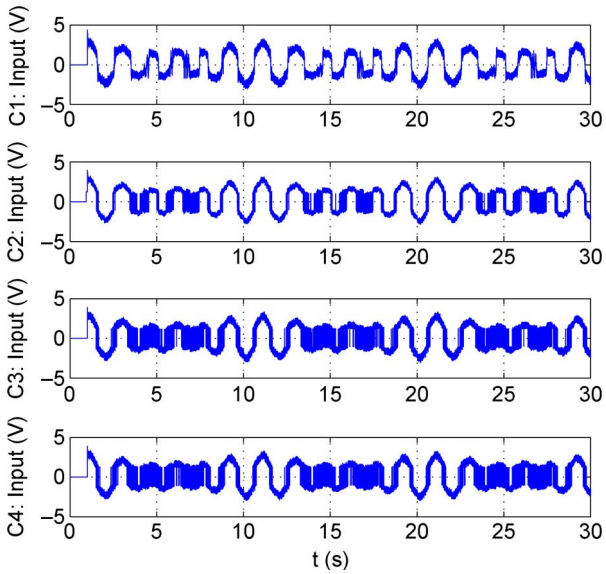

Fig. 7. Control input history of DIARCs with dead-zone.

four cases, and it is observed that all four cases have good initial output tracking transient performance, illustrating the strong robust transient performance of the proposed DIARC strategy in general. It is also seen that the steady-state output tracking errors of C3 and C4 are almost the same and on the order of $10^{-6}m$, which are much less than that of C2 that is on the order of $10^{-5}m$. This result agrees with the prediction by theory in Section III that the proposed DIARC in C3 is able to achieve asymptotic convergence of dead-zone parameter estimates to their true values and the perfect dead-zone compensation of the proposed dead-zone inverse (4) when the estimates converge. This is also revealed by the history of system parameter estimates in Fig. 5. Furthermore, C2, C3, and C4 have much better output tracking performances than C1, which illustrates the necessity of dead-zone compensation. The estimate values of $\widehat{B} = 0.78$, $\widehat{A} = 0.23$, and $\widehat{E} = 1.58$ shown in Fig. 6 are close to their offline identified values, and the estimated values of $\widehat{\theta} = [0.82, 0.225, 1.42, 1.66, 1.5, -1.49]^{\mathrm{T}}$ shown in Fig. 5 are near the approximate accurate value of θ, which verify the asymptotic convergence of system parameter estimates as well. The control inputs of all four cases shown in Fig. 7 reveal that the control input may exhibit some chattering phenomena during periods when the motion is very small and the system is almost operating within the dead-zone region due to the use of the nonsmooth direct dead-zone inverse (4). In summary, the good output tracking performance of all four cases demonstrates the robust performance of the proposed DIARC algorithm. The much-improved output tracking performances of C2, C3, and C4 over C1 illustrate the necessity of dead-zone compensation. The much-improved steady-state tracking performance of C3 over C2 validates the need for accurate online dead-zone parameter estimates. Moreover, the almost similar asymptotically converging steady-state output tracking performances of C3 and C4 verify the asymptotic convergence of dead-zone parameter estimates to their true values and further validate the perfect compensation of unknown dead-zones by the proposed DIARC algorithm.

B. Comparative Experiment II

To further illustrate the effectiveness and merits of the proposed scheme, the robust adaptive control algorithm proposed in [18], a typical example of the previously published algorithms for systems with dead-zones, is also implemented for comparison. As the control algorithm in [18] is designed for systems with symmetric dead-zones only, in the following, the simulated dead-zone is set as equal slope and described by

$$w = D(v) = \begin{cases} 1.395v - 1.674, & \text{for } v \geq 1.2 \\ 0, & \text{for } -1 < v < 1.2 \\ 1.395v + 1.395, & \text{for } v \leq -1. \end{cases} \quad (39)$$

Thus, the approximate accurate values are $\theta = [0.8, 0.23, 1.395, 1.674, 1.395, -1.395]^{\mathrm{T}}$. The bounds of the parametric variations are chosen as similar as that of (38).

The proposed DIARC referred to as C3 and the robust adaptive control algorithm (presented in [18]) referred to as C5 are implemented and compared. For C3, the control parameters and the initial values are the same as those in Section IV-A.

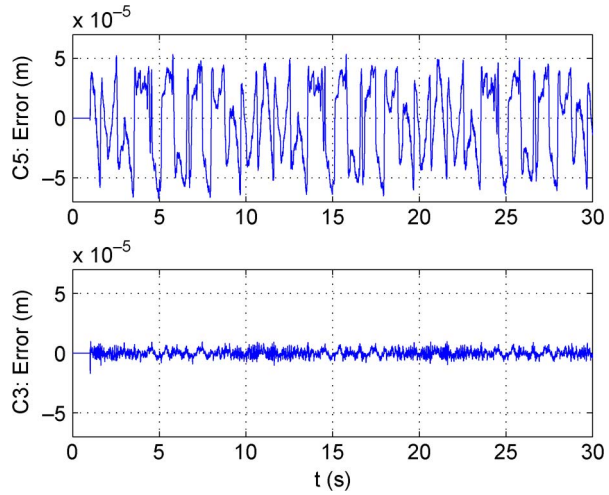

Fig. 8. Output tracking errors of C5 and C3 with dead-zone.

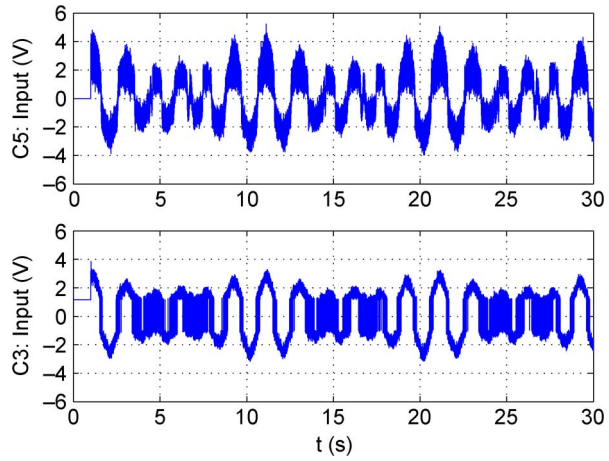

Fig. 9. Control input history of C5 and C3 with dead-zone.

For C5, the control law is designed following exactly the same procedure in [18]

$$v = \widehat{e} w_d$$

$$w_d = \ddot{x}_d(t) - c_1 \dot{z}_1 - \varphi \widehat{\theta}_p - c_2 z_2 - z_1 - sgn(z_2)\widehat{D}$$

$$\dot{\widehat{e}} = -\beta w_d z_2 \quad \dot{\widehat{\theta}}_p = \Gamma \varphi^T z_2 \quad \dot{\widehat{D}} = \mu |z_2| \tag{40}$$

where $z_1 = \widetilde{x}(t)$, $z_2 = \dot{z}_1 + c_1 z_1$, $c_1 = 100$, $c_2 = 120$, $\mu = 1000$, $\Gamma = 10 I_2$, and $\beta = 10$. The initial values are $\widehat{e}(0) = 1/1.4$, $\widehat{D}(0) = 0$, $\widehat{\theta}_p(0) = [0.8, 0.23]^{\mathrm{T}}$, and $v(0) = 0$.

The experimental results in terms of some performance indexes after running the gantry for one period are given in Experiment II of Table I. It can be seen from these results that the proposed DIARC algorithm outperforms the robust adaptive control algorithm in [18] significantly. The experimental results for the two controllers are also shown in Fig. 8 in terms of the output tracking performance and in Fig. 9 for the control inputs. It is seen from Fig. 8 that the steady-state output tracking error of the proposed DIARC is mostly less than 10 μm and around zero, which is much less than that of C5 that does not exhibit a near-zero tracking error during most of the movements. This result verifies the asymptotical output tracking performance of the proposed DIARC in the presence of parametric uncertainties and unknown dead-zones. The control inputs shown in Fig. 9 reveal that the robust adaptive control algorithm in [18] exhibits the control input chattering phenomena during the entire motion due to the use of discontinuous control action (the last term in w_d in (40)), while the proposed DIARC only has the chattering input during periods when the motion is very small and the system is essentially operating at the dead-zone region only. All these results further validate the effectiveness and the high-performance nature of the proposed DIARC algorithm.

V. Conclusion

In this paper, an integrated direct/indirect desired compensation adaptive robust control scheme has been developed for electrical drive systems having unknown dead-zone effects. The proposed control strategy, in which the actual state feedback in the regressor is replaced by the precalculated desired trajectory, is able to reduce the effects of measurement noise for an increased achievable closed-loop bandwidth in application. Theoretically, certain guaranteed robust transient performance and steady-state tracking accuracy are achieved even when the overall system may be subjected to parametric uncertainties, time-varying disturbances, and other uncertain nonlinearities. Furthermore, zero steady-state output tracking error is achieved when the system is subjected to unknown parameters and unknown dead-zone only. Comparative experimental results have been obtained on a linear motor drive system preceded by a simulated unknown dead-zone. The results validate the effectiveness of the proposed dead-zone compensation scheme, and the excellent output tracking performances also verify the high-performance nature of the proposed DIARC strategy in practical applications.

Appendix A

Proof of Lemma 1: It is noted from (6) that $\kappa_+(w_d) + \kappa_-(w_d) = 1\ \forall w_d$. Thus, there are only two cases to be examined: **Case 1**: $\kappa_+(w_d) = 1$ and $\kappa_-(w_d) = 0$, and **Case 2**: $\kappa_-(w_d) = 1$ and $\kappa_+(w_d) = 0$.

Case 1) $w_d(t) \geq 0$, and by (4), $v(t) = (w_d(t) + \widehat{(m_r b_r)}/\widehat{m_r}) > 0$.

If $v(t) \geq b_r$, then, by (2), $w(t)$ can be derived as $w(t) = m_r v - m_r b_r = m_r(w_d + \widehat{(m_r b_r)}/\widehat{m_r}) - m_r b_r = w_d + \widetilde{(m_r b_r)} - \widetilde{m_r}(w_d + \widehat{(m_r b_r)}/\widehat{m_r})$. Noting (7), $d(t) = 0$, which leads to the first scenario of (8).

If $0 < v < b_r$, from (2), $w(t) = 0$. Thus, by (7)

$$d(t) = -w_d - \widetilde{(m_r b_r)} + \widetilde{m_r}\frac{w_d + \widehat{(m_r b_r)}}{\widehat{m_r}}$$

$$= m_r b_r - \frac{w_d + \widehat{(m_r b_r)}}{\widehat{m_r}} m_r \tag{41}$$

which leads to the second scenario of (8). Furthermore, as $0 \le w_d(t) = \widehat{m_r} v - \widehat{(m_r b_r)} < \widehat{m_r} b_r - \widehat{(m_r b_r)}$, $d(t)$ in (41) satisfies

$$d(t) \in \left(0, m_r b_r - m_r \frac{\widehat{(m_r b_r)}}{\widehat{m_r}}\right] \tag{42}$$

which leads to the upper bound in the second scenario of (9).

Case 2) As the same can be said about this case, (7) and (8) are validated, and $d(t)$ is bounded previously as in (9).

Note that (42) is the same as $d(t) \in (0, -\widetilde{(m_r b_r)} + \widetilde{m_r}(\widehat{(m_r b_r)}/\widehat{m_r})]$. Thus, $\forall t$, $|d(t)| \le \max\{|\widetilde{(m_r b_r)}| + |\widetilde{m_r}|((m_r b_r)_{\max}/m_{rmin}), |\widetilde{(m_l b_l)}| + |\widetilde{m_l}|(|(m_l b_l)_{\min}|/m_{lmin})\}$. Since $\widetilde{\theta} \in L_2[0,\infty)$ implies that $\widetilde{(m_r b_r)}$, $\widetilde{m_r}$, $\widetilde{(m_l b_l)}$, $\widetilde{m_l} \in L_2[0,\infty)$, it is clear that $\widetilde{\theta} \in L_2[0,\infty)$ leads to $d(t) \in L_2[0,\infty)$ as well. Similarly, it is true that $\widetilde{\theta}(t) \to 0$ ensures $d(t) \to 0$ as $t \to \infty$, which completes the proof. ■

APPENDIX B

Proof of Theorem 1: Noting (19), the derivative of V_s is

$$\begin{aligned}\dot{V}_s &= (-B - Ag)\dot{\widetilde{x}} s + k^\star w_{ds1} s \\ &\quad + s\left[k^\star w_{ds2} - \widetilde{d}_c + (1-k^\star)\widehat{d}_c + \triangle^\star(t)\right] + \lambda^2 \widetilde{x}\dot{\widetilde{x}}. \end{aligned} \tag{43}$$

Noting 2) of (20) and $\dot{\widetilde{x}} = s - \lambda\widetilde{x}$, we have

$$\dot{V}_s \le (-k^\star k_{s1} - B - Ag)s^2 + (B + Ag + \lambda)\lambda\widetilde{x}s - \lambda^3\widetilde{x}^2 + \varepsilon + \varepsilon_d f_d^2. \tag{44}$$

If Q_1 given by (15) is positive definite, then

$$\dot{V}_s \le -k_2 s^2 - \frac{1}{2}\lambda^3\widetilde{x}^2 + \varepsilon + \varepsilon_d f_d^2 \le -\lambda_v V_s + \varepsilon + \varepsilon_d f_d^2. \tag{45}$$

Using the comparison lemma, (23) is true. The theorem can then be proved by noting that all online parameter estimates are guaranteed to be bounded regardless of the estimation function to be used shown in P1). ■

APPENDIX C

Proof of Lemma 2: When $w_d(t) \ge H$, noting (4) and the bounds of the dead-zone parameter estimates in P1), $v(t) = (w_d(t) + \widehat{(m_r b_r)}/\widehat{m_r}) \ge (H + \widehat{(m_r b_r)}/\widehat{m_r}) \ge ((m_r b_r)_{\max}/\widehat{m_r}) \ge b_r$. When $w_d(t) \le -H$, it is straightforward to verify that $v(t) = (w_d(t) + \widehat{(m_l b_l)}/\widehat{m_l}) \le ((m_l b_l)_{\min}/\widehat{m_l}) \le b_l$, which completes the proof. ■

APPENDIX D

Proof of Theorem 2: When the PE condition is satisfied, from Lemma 3, $\widetilde{\theta}_b(k) \to 0$ as $k \to \infty$ and $\widetilde{\theta}_b \in l_2$. Thus, noting Lemma 1, we have $d(t) \in L_2[0,\infty)$ as well.

Noting (14) and (16), the derivative of V_s when $f_u = 0$ is

$$\dot{V}_s = (-B - Ag)\dot{\widetilde{x}} s + k^\star w_{ds} s - \widehat{d}_c s + d(t)s + \xi s + \lambda^2 \widetilde{x}\dot{\widetilde{x}} \tag{46}$$

where

$$\begin{aligned}\xi &= \left[\left(\frac{\widetilde{m_r}}{\widehat{m_r}}\widehat{d}_c - \frac{\widetilde{m_r}}{\widehat{m_r}} w_{da1}\right)\kappa_+(w_d) \right. \\ &\quad \left. + \left(\frac{\widetilde{m_l}}{\widehat{m_l}}\widehat{d}_c - \frac{\widetilde{m_l}}{\widehat{m_l}} w_{da1}\right)\kappa_-(w_d) - \varphi_d \widetilde{\theta}_p\right] \\ &\quad + \left(\widetilde{(m_r b_r)} - \widetilde{m_r}\frac{\widehat{(m_r b_r)}}{\widehat{m_r}}\right)\kappa_+(w_d) \\ &\quad + \left(\widetilde{(m_l b_l)} - \widetilde{m_l}\frac{\widehat{(m_l b_l)}}{\widehat{m_l}}\right)\kappa_-(w_d). \end{aligned} \tag{47}$$

Choose a positive definite function as $V_a = V_s + (1/2\gamma)\widehat{d}_c^{\,2}$. Then, noting $\dot{\widetilde{x}} = s - \lambda\widetilde{x}$ and $Q_1 > 0$, we have

$$\begin{aligned}\dot{V}_a &= \dot{V}_s + \gamma^{-1}\widehat{d}_c\dot{\widehat{d}}_c \\ &= (-k^\star k_{s1} - B - Ag)\, s^2 + (B + Ag + \lambda)\lambda\widetilde{x}s - \lambda^3\widetilde{x}^2 \\ &\quad + k^\star w_{ds2} s + d(t)s + \xi s + \left(\gamma^{-1} Proj_{\widehat{d}_c}(\gamma s) - s\right)\widehat{d}_c \\ &\le -k_2 s^2 - \frac{1}{2}\lambda^3\widetilde{x}^2 + k^\star w_{ds2} s + d(t)s + \xi s \end{aligned} \tag{48}$$

where (11) of P2) is used in deriving the inequality of the last step. As ξ defined by (47) is linear w.r.t. the parameter estimation error $\widetilde{\theta}$, with all coefficients being uniformly bounded by Theorem 1, the fact that $\widetilde{\theta} \in l_2$ implies that $\xi \in L_2[0,\infty)$. From 1) of (20), $k^\star w_{ds2} s \le 0$. Thus, (48) implies that $s \in L_2[0,\infty)$ as $\xi \in L_2[0,\infty)$ and $d(t) \in L_2[0,\infty)$. It is easy to verify that s is uniformly continuous. Thus, by Barbalat's lemma, $s \to 0$ as $t \to \infty$. Noting (12), $\widetilde{X}(t) \to 0$ as $t \to \infty$, which completes the proof. ■

REFERENCES

[1] Y. Tan, R. Dong, and R. Li, "Recursive identification of sandwich systems with dead zone and application," *IEEE Trans. Control Syst. Technol.*, vol. 17, no. 4, pp. 945–951, Jul. 2009.

[2] T. Chang, D. Yuan, and H. Hanek, "Matched feedforward/model reference control of a high precision robot with dead-zone," *IEEE Trans. Control Syst. Technol.*, vol. 16, no. 1, pp. 94–102, Jan. 2008.

[3] H. Liaw and B. Shirinzadeh, "Robust adaptive constrained motion tracking control of piezo-actuated flexure-based mechanisms for micro/nano manipulation," *IEEE Trans. Ind. Electron.*, 2010, doi: 10.1109/TIE.2010.2050413.

[4] S. Huang, K. K. Tan, and T. H. Lee, "Adaptive sliding-mode control of piezoelectric actuators," *IEEE Trans. Ind. Electron.*, vol. 56, no. 9, pp. 3514–3522, Sep. 2009.

[5] M. Ruderman, F. Hoffmann, and T. Bertram, "Modeling and identification of elastic robot joints with hysteresis and backlash," *IEEE Trans. Ind. Electron.*, vol. 56, no. 10, pp. 3840–3847, Oct. 2009.

[6] S. Villwock and M. Pacas, "Time-domain identification method for detecting mechanical backlash in electrical drives," *IEEE Trans. Ind. Electron.*, vol. 56, no. 2, pp. 568–573, Feb. 2009.
[7] Z. Jamaludin, H. Van Brussel, and J. Swevers, "Friction compensation of an XY feed table using friction-model-based feedforward and an inverse-model-based disturbance observer," *IEEE Trans. Ind. Electron.*, vol. 56, no. 10, pp. 3848–3853, Oct. 2009.
[8] C. Y. Lai, F. L. Lewis, V. Venkataramanan, X. Ren, S. S. Ge, and T. Liew, "Disturbance and friction compensations in hard disk drives using neural networks," *IEEE Trans. Ind. Electron.*, vol. 57, no. 2, pp. 784–792, Feb. 2010.
[9] G. Tao and F. L. Lewis, *Adaptive Control of Nonsmooth Dynamic Systems*. New York: Springer-Verlag, 2001.
[10] G. Tao and P. V. Kokotovic, "Adaptive control of plants with unknown dead-zones," *IEEE Trans. Autom. Control*, vol. 39, no. 1, pp. 59–68, Jan. 1994.
[11] J. O. Jang, "Deadzone compensation of an XY-positioning table using fuzzy logic," *IEEE Trans. Ind. Electron.*, vol. 52, no. 6, pp. 1696–1701, Dec. 2005.
[12] R. R. Selmic and F. L. Lewis, "Dead-zone compensation in motion control systems using neural networks," *IEEE Trans. Autom. Control*, vol. 45, no. 4, pp. 602–613, Apr. 2000.
[13] X.-S. Wang, C.-Y. Su, and H. Hong, "Robust adaptive control of a class of linear systems with unknown dead-zone," *Automatica*, vol. 40, pp. 407–413, 2004.
[14] S. Ibrir, W. F. Xie, and C.-Y. Su, "Adaptive tracking of nonlinear systems with non-symmetric dead-zone input," *Automatica*, vol. 43, no. 3, pp. 522–530, Mar. 2007.
[15] T. Zhang and S. S. Ge, "Adaptive neural network tracking control of MIMO nonlinear systems with unknown dead zones and control directions," *IEEE Trans. Neural Netw.*, vol. 20, no. 3, pp. 483–497, Mar. 2009.
[16] J. Zhou, C. Wen, and Y. Zhang, "Adaptive output control of nonlinear systems with uncertain dead-zone nonlinearity," *IEEE Trans. Autom. Control*, vol. 51, no. 3, pp. 504–511, Mar. 2006.
[17] C. Hu, B. Yao, and Q. Wang, "Integrated direct/indirect adaptive robust control of a class of nonlinear systems preceded by unknown dead-zone nonlinearity," in *Proc. 48th IEEE Conf. Decision Control*, Shanghai, China, Dec. 2009, pp. 6626–6631.
[18] J. Zhou, C. Wen, and Y. Zhang, "Adaptive backstepping control of a class of uncertain nonlinear systems with unknown backlash-like hysteresis," *IEEE Trans. Autom. Control*, vol. 49, no. 10, pp. 1751–1757, Oct. 2004.
[19] O. Kaynak, K. Erbatur, and M. Ertugrul, "The fusion of computationally intelligent methodologies and sliding-mode control—A survey," *IEEE Trans. Ind. Electron.*, vol. 48, no. 1, pp. 4–17, Feb. 2001.
[20] X. Yu and O. Kaynak, "Sliding-mode control with soft computing: A survey," *IEEE Trans. Ind. Electron.*, vol. 56, no. 9, pp. 3275–3285, Sep. 2009.
[21] B. Yao and M. Tomizuka, "Smooth robust adaptive sliding mode control of robot manipulators with guaranteed transient performance," *Trans. ASME, J. Dyn. Syst. Meas. Control*, vol. 118, no. 4, pp. 764–775, Dec. 1996.
[22] L. Xu and B. Yao, "Adaptive robust precision motion control of linear motors with negligible electrical dynamics: Theory and experiments," *IEEE/ASME Trans. Mechatronics*, vol. 6, no. 4, pp. 444–452, Dec. 2001.
[23] B. Yao, "Desired compensation adaptive robust control," *Trans. ASME, J. Dyn. Syst. Meas. Control*, vol. 131, no. 6, pp. 061001-1–061001-7, Nov. 2009.
[24] B. Yao, "Integrated direct/indirect adaptive robust control of SISO nonlinear systems in semi-strict feedback form," in *Proc. Amer. Control Conf.*, Denver, CO, Jun. 2003, pp. 3020–3025.
[25] B. Yao, "High performance adaptive robust control of nonlinear systems: A general framework and new schemes," in *Proc. IEEE Conf. Decision Control*, San Diego, CA, 1997, pp. 2489–2494.
[26] M. Krstic, I. Kanellakopoulos, and P. V. Kokotovic, *Nonlinear and Adaptive Control Design*. New York: Wiley, 1995.
[27] C. Hu, B. Yao, and Q. Wang, "Integrated direct/indirect adaptive robust contouring control of a biaxial gantry with accurate parameter estimations," *Automatica*, vol. 46, no. 4, pp. 701–707, Apr. 2010.
[28] I. D. Landau, R. Lozano, and M. M'Saad, *Adaptive Control*. New York: Springer-Verlag, 1998.
[29] C. Hu, B. Yao, and Q. Wang, "Coordinated adaptive robust contouring controller design for an industrial biaxial precision gantry," *IEEE/ASME Trans. Mechatronics*, vol. 15, no. 5, pp. 728–735, Oct. 2010.
[30] C. Hu, B. Yao, and Q. Wang, "Coordinated adaptive robust contouring control of an industrial biaxial precision gantry with cogging force compensations," *IEEE Trans. Ind. Electron.*, vol. 57, no. 5, pp. 1746–1754, May 2010.

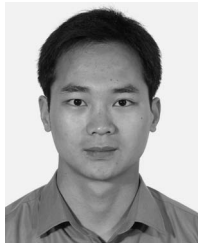

Chuxiong Hu (S'09) received the B.Eng. and Ph.D. degrees in mechanical engineering from Zhejiang University, Hangzhou, China, in 2005 and 2010, respectively.

From 2007 to 2008, he was a Visiting Scholar in mechanical engineering at Purdue University, West Lafayette, IN. He is currently a Postdoctoral Researcher with the Department of Precision Instruments and Mechanology, Tsinghua University, Beijing, China. His research interests include high-performance multiaxis motion control, precision mechatronic systems and measurements, adaptive and robust control, and nonlinear systems.

Bin Yao (S'92–M'96–SM'09) received the B.Eng. degree in applied mechanics from the Beijing University of Aeronautics and Astronautics, Beijing, China, in 1987, the M.Eng. degree in electrical engineering from Nanyang Technological University, Singapore, Singapore, in 1992, and the Ph.D. degree in mechanical engineering from the University of California, Berkeley, in 1996.

He has been with the School of Mechanical Engineering, Purdue University, West Lafayette, IN, since 1996 and was promoted to the rank of Professor in 2007. He became a Kuang-Piu Professor and a Chang Jiang Chair Professor at Zhejiang University, Hangzhou, China, in 2005 and 2010, respectively.

Dr. Yao was awarded the Faculty Early Career Development (CAREER) Award from the National Science Foundation in 1998 and the Joint Research Fund for Outstanding Overseas Chinese Young Scholars from the National Natural Science Foundation of China in 2005. He was also the recipient of the O. Hugo Schuck Best Paper (Theory) Award from the American Automatic Control Council in 2004 and the Outstanding Young Investigator Award of the American Society of Mechanical Engineers (ASME) Dynamic Systems and Control Division (DSCD) in 2007. He has chaired numerous sessions and served in the International Program Committee of various IEEE, ASME, and International Federation of Automatic Control conferences. From 2000 to 2002, he was the Chair of the Adaptive and Optimal Control Panel, and from 2001 to 2003, he was the Chair of the Fluid Control Panel of ASME DSCD. He is currently the Vice-Chair of the ASME DSCD Mechatronics Technical Committee. He was the Technical Editor of the IEEE/ASME TRANSACTIONS ON MECHATRONICS from 2001 to 2005 and has been the Associate Editor of the *ASME Journal of Dynamic Systems, Measurement, and Control* since 2006.

Qingfeng Wang received the M.Eng. and Ph.D. degrees in mechanical engineering from Zhejiang University, Hangzhou, China, in 1988 and 1994, respectively.

He then became a Faculty Member at Zhejiang University, where he was promoted to the rank of Professor in 1999. He was the Director of the State Key Laboratory of Fluid Power Transmission and Control, Zhejiang University, from 2001 to 2005 and is currently the Director of the Institute of Mechatronic Control Engineering. His research interests include electrohydraulic control components and systems, hybrid power system and energy-saving technique for construction machinery, and system synthesis for mechatronic equipment.